Clinical Immunology 264 (2024) 110261

Contents lists available at ScienceDirect

Clinical Immunology

journal homepage: www.elsevier.com/locate/yclim

A proximal enhancer regulates RORA expression during early human Th17 cell differentiation

Ubaid Ullah Kalim [a,b,*,1], Rahul Biradar [a,b,1], Sini Junttila [a,b], Mohd Moin Khan [a], Subhash Tripathi [a], Meraj Hasan Khan [a], Johannes Smolander [a,b], Kartiek Kanduri [a], Tapio Envall [a], Asta Laiho [a,b], Alexander Marson [c,d], Omid Rasool [a,b], Laura L. Elo [a,b,e], Riitta Lahesmaa [a,b,e,*]

[a] Turku Bioscience Centre, University of Turku and Åbo Akademi University, Turku, Finland
[b] InFLAMES Research Flagship Center, University of Turku, Turku, Finland
[c] Gladstone-UCSF Institute of Genomic Immunology, San Francisco, CA 94158, USA
[d] Department of Medicine, University of California San Francisco, San Francisco, CA 94143, USA
[e] Institute of Biomedicine, University of Turku, Turku, Finland

ARTICLE INFO

Keywords:
Enhancer mapping
Human Th17 cells
Autoimmunity
Regulatory SNPs
RORA

ABSTRACT

Gene regulatory elements, such as enhancers, greatly influence cell identity by tuning the transcriptional activity of specific cell types. Dynamics of enhancer landscape during early human Th17 cell differentiation remains incompletely understood. Leveraging ATAC-seq-based profiling of chromatin accessibility and comprehensive analysis of key histone marks, we identified a repertoire of enhancers that potentially exert control over the fate specification of Th17 cells. We found 23 SNPs associated with autoimmune diseases within Th17-enhancers that precisely overlapped with the binding sites of transcription factors actively engaged in T-cell functions. Among the Th17-specific enhancers, we identified an enhancer in the intron of RORA and demonstrated that this enhancer positively regulates RORA transcription. Moreover, CRISPR-Cas9-mediated deletion of a transcription factor binding site-rich region within the identified RORA enhancer confirmed its role in regulating RORA transcription. These findings provide insights into the potential mechanism by which the RORA enhancer orchestrates Th17 differentiation.

1. Introduction

Interleukin-17-producing T helper (Th) cells (Th17) play a pivotal role in the host response to a variety of infections and also contribute to the pathogenesis of several autoimmune and inflammatory diseases. Th17 cell differentiation occurs when a naive $CD4^+$ T cell is activated in the presence of an inflammatory milieu containing IL-6 and IL-1β [1]. This differentiation process is initiated by signaling through cytokine receptors and transcription factors (TFs) that orchestrate gene regulation *via* gene regulatory elements, such as promoters and enhancers. These early events are followed by dynamic changes in the epigenetic landscape of the cells, including alterations in chromatin accessibility and histone modifications. While the cytokines, signaling intermediates and transcriptional changes associated with Th17 cell differentiation have been meticulously elucidated [1–6], our understanding of the epigenetic regulation of Th17 cell differentiation in humans remains limited.

Regulatory elements, such as enhancers, regulate gene expression in *cis* by bringing TF complexes onto the promoter of specific genes. Enhancers are cell type specific and dynamically formed during cell development and differentiation. They are often associated with monomethylation of fourth lysine residue on the histone-three tail (H3K4me1). The active enhancers are further marked by acetylation marks at 27th lysine of histone-three tail (H3K27ac).

Enhancer landscape of mouse Th17 cells using histone acetyltransferase p300 binding data [7] or TF co-occupancy data has been reported [8]. Additionally, studies utilizing chromatin accessibility analysis, in conjunction with histone modification data, have revealed

* Corresponding authors at: Turku Bioscience Centre, University of Turku and Åbo Akademi University, Turku, Finland.
E-mail addresses: ubaull@utu.fi (U.U. Kalim), rilahes@utu.fi (R. Lahesmaa).
[1] These authors contributed equally to this work

https://doi.org/10.1016/j.clim.2024.110261
Received 10 January 2024; Received in revised form 19 April 2024; Accepted 21 May 2024
Available online 22 May 2024

gene regulatory networks that govern murine Th17 cell differentiation [9]. Notably, a proximal enhancer has been shown to promote the expression of RAR-related Orphan Receptor-γt (RORγt), a key TF in Th17 cells, during experimental autoimmune encephalomyelitis (EAE), a mouse model of multiple sclerosis [10]. While the enhancer landscape of mouse Th17 cells has been studied, the corresponding understanding of human Th17 cells, particularly during early differentiation stages, remains unexplored.

A study on chromatin dynamics during hematopoiesis identified threefold more enhancers than promoters, underscoring the early establishment of enhancers during lineage commitment [11]. Therefore, enhancers in terminally differentiated cells are expected to differ from those of the cells undergoing differentiation [12], highlighting the importance of studying enhancers during early Th17 cell differentiation. A comprehensive map of these cell-type-specific regulatory elements and their interplay with lineage-specific TF networks can provide critical insights into potential epigenetic alterations that may contribute to autoimmune disorders by exacerbating the Th17 response.

Remarkably, over 90% of disease associated single nucleotide polymorphisms (SNPs) are located within noncoding regulatory regions, including enhancers [13]. Earlier, we showed that enhancers associated with human Th1 and Th2 cells overlapped significantly with the autoimmune disease–associated SNPs [12]. Autoimmune disease–associated SNPs within enhancers, particularly those that are near binding sites of TFs, may affect TF binding and gene transcription.

In this study, we identified and studied enhancer elements that shape the transcriptional landscape of cells polarizing towards Th17 lineage. Further, we studied the enrichment of autoimmune disease-associated SNPs within the enhancer elements. We found an enhancer region near RORA gene that was specific to Th17 cells. RAR-related orphan receptors RORγt (encoded by *RORC*) and RORα (encoded by *RORA*) contribute to Th17 differentiation [14], and their target genes during the process have been characterized [7,15]. However, much less is known about the contribution of *cis*-regulatory elements in regulating these factors. Additionally, using CRISPR-Cas9-mediated deletion of an enhancer near RORA coupled with functional luciferase assay, we analyzed the effect of enhancer deletion on the expression of *RORA* and *IL17A* during early human Th17 cell differentiation.

2. Results

2.1. Chromatin accessibility is dynamic during early human Th17 cell differentiation

Chromatin accessibility is a key feature regulating gene expression. To unravel the chromatin accessibility landscape of early differentiating human Th17 cells, we used Assay for Transposase-Accessible Chromatin with high-throughput sequencing (ATAC-seq) analysis. Samples were collected at 0, 2, 4, 24, 48 and 72 h during early Th17 cell development, as well as control cells activated in the absence of any polarizing cytokines (Th0) (Fig. 1A). Th17 differentiation was confirmed by high levels of CCR6 surface expression (Fig. 1B) and high IL-17A expression at RNA (Fig. 1C) and protein (Fig. 1D) levels. After normalization, the ATAC-seq data showed little variation (Fig. S1A). The biggest difference in chromatin openness was observed between early and late time points, both in activated (Th0) and Th17 cells. Further, although the ATAC-seq profiles of the Th0 and Th17 cells were close to each other at early time points, the difference became greater as the cells progressed further through the differentiation (Fig. S1B). Using an irreproducible discovery rate (IDR) threshold of 0.05, we found approximately 20,000 peaks at each time point during Th17 differentiation (Fig. S1C) of which 1618–7278 peaks were unique to Th17 cells at different time points (Fig. 1E).

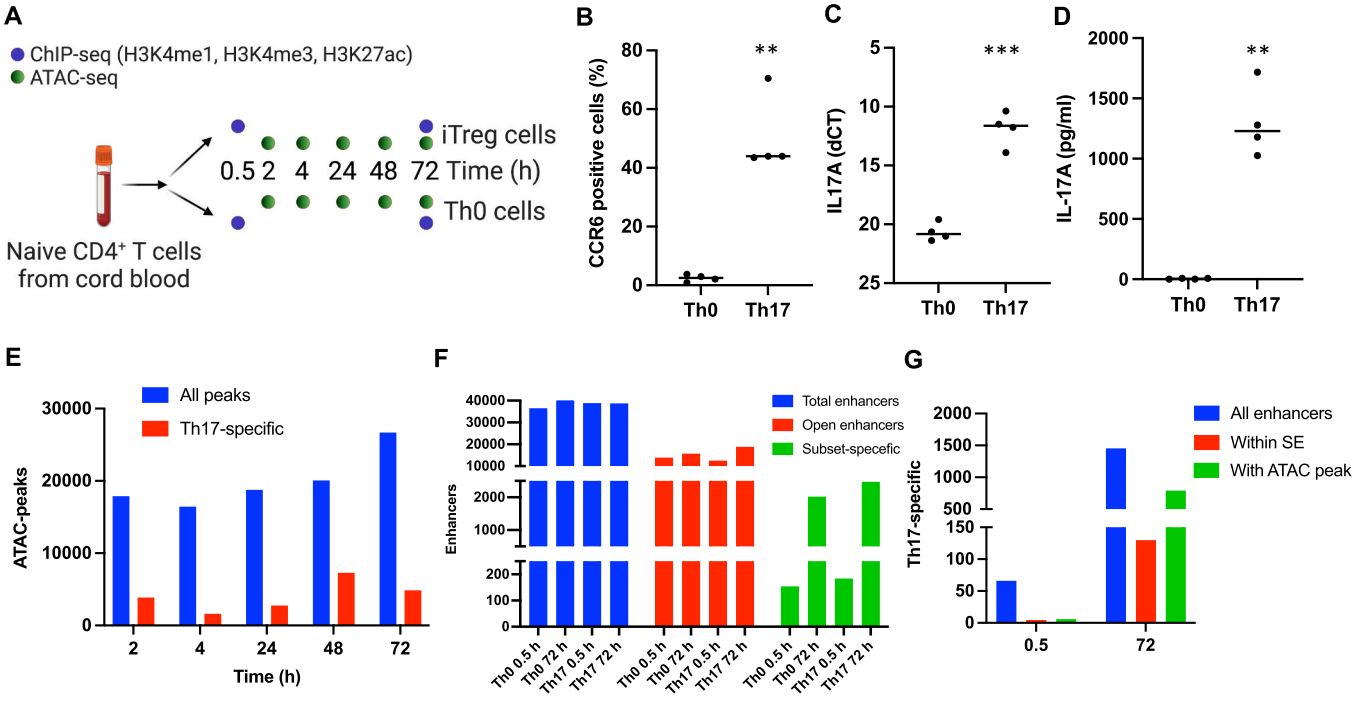

Fig. 1. Identification of Th17-specific enhancers. (A) Overview of experimental design. Created with Biorender.com. (B) Percentage CCR6 positive cells at 72 h of differentiation in Th0 and Th17 cells. (C) IL17 A mRNA expression in Th0 and Th17 cells at 72 h. The expression is plotted relative to EF1A. (D) IL-17A secretion in the culture supernatant in Th0 and Th17 cells at 72 h. (B–D) Each dot is an individual biological replicate and the horizontal line shows the mean. Statistical significance was determined using two-tailed paired *t*-test. **:$p < 0.01$, ***:$p < 0.001$. (E) ATAC-seq open chromatin regions during Th17 differentiation at the indicated time points. (F) Total enhancers (blue), enhancers containing ATAC-peaks (red) and subset-specific enhancers (green) identified in Th0 and Th17 cells at 0.5 and 72 h. (G) Th17-specific enhancers at 0.5 and 72 h, where Th1/Th2 enhancers from Hawkins et al. (2013) have been excluded. (For interpretation of the references to color in this figure legend, the reader is referred to the web version of this article.)

2.2. Histone profiling coupled with machine learning identifies Th17-specific enhancers during early human Th17 cell differentiation

To determine the enhancer landscape of early human Th17 cell differentiation, we used ChIP-seq to profile H3K4me1, H3K4me3, and H3K27ac histone marks at 0.5 and 72 h during differentiation (Fig. 1A). We used a Hidden Markov Model (HMM)-based ChromHMM machine learning tool [16] to predict the enhancers from the histone modification data. The workflow of the analysis is shown in Fig. S2A. Based on histone modification data, we classified the chromatin into five states: weak enhancer; strong enhancer; weak promoter; strong promoter; and heterochromatin (Fig. S2B-C).

We detected 38,861 and 38,735 enhancers in differentiating Th17 cells at 0.5 and 72 h, respectively. Similarly, we observed 36,506 and 43,554 enhancers in Th0 cells at 0.5 and 72 h, respectively (Fig. 1F). The majority of the enhancers were intronic followed by intergenic and promoter-overlapping enhancers (Fig. S2D). By overlapping ChIP-seq and ATAC-seq peaks, we found that about a third of the enhancers had accessible chromatin (Fig. 1F). While only 154 and 184 enhancers were specific to Th0 or Th17 cells, respectively at 0.5 h, the number of unique enhancers at 72 h was 2020 and 2473 in the two cell types, respectively (Fig. 1F). To identify Th17-specific enhancers, we excluded the enhancers we reported earlier in Th1 and Th2 cells [12], and identified 66 and 1453 enhancers unique to early Th17 cells at 0.5 and 72 h, respectively, of which 6 and 792, respectively, had open chromatin loci within them. Clusters of enhancers having high density of transcription factor binding sites (TFBS), often referred to as super-enhancers (SE), tend to be more efficient in enhancing the transcription than single enhancers [17]. Among the 66 and 1453 Th17-specific enhancers at the two time points, 4 and 130 were part of a SE region, respectively (Fig. 1G and Table S1). Interestingly, of the 66 and 1453 Th17 enhancers at the two time points, 3 and 22, respectively, overlapped with the enhancers active in the cells of human colon biopsy samples from inflammatory bowel disease (IBD) patients [18], suggesting that these enhancers may contribute to the pathology. From the GeneHancer database [19], these Th17-specific enhancers were predicted to interact with 70 and 1631 promoters, respectively (Table S2).

2.3. Th17-specific enhancers were associated with increased expression of neighboring genes

To study enhancer-gene associations, we analyzed the expression of genes near the Th17-specific enhancers during early Th17 differentiation using RNA-seq data from our earlier study [20]. While only four genes (*ITGA1*, *NUDCD1*, *FBX015*, and *FRY*) were differentially expressed (DE) among the genes in the vicinity of the enhancers identified at 0.5 h, there were 155 DE genes in the vicinity of the 72 h enhancers (Fig. 2). Interestingly, 140 of the 155 genes were upregulated during early Th17 cell differentiation, indicating that the enhancers were more often associated with upregulation than downregulation of the transcription.

2.4. Th17-cell-associated TFs were enriched within the enhancers

Next, we tested the enrichment of 658 TFBS motifs corresponding to the TFs expressed in Th17 cells [20] within the Th17-specific enhancers at the two time points: 257 and 445 TFBS were enriched within 0.5 and 72 h enhancers, respectively (Table S3). The high degree of TFBS enrichment indicates that these enhancers are transcriptionally active TFBS-rich regions. Interestingly, TFBS for STAT3, RORγt and RORα were enriched only within 72 h enhancers but not within 0.5 h enhancers.

2.5. Autoimmune disease–associated SNPs were enriched near Th17-specific enhancers

We determined if disease-associated SNPs were enriched near Th17-specific enhancers. We used the snpEnrichR tool to examine 11

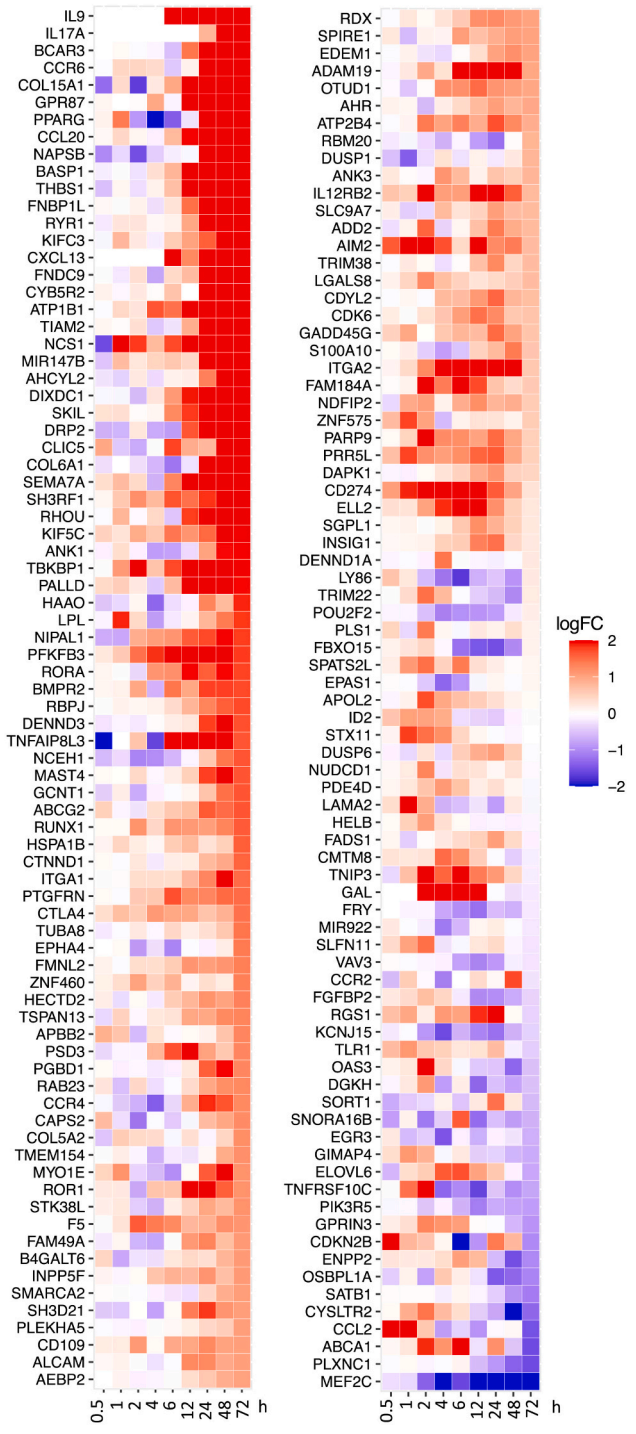

Fig. 2. Enhancers were more often associated with upregulation than downregulation of transcription. The heatmap shows the expression of genes near Th17-specific enhancers under Th17 conditions. The expression data are taken from Tuomela et al. (2016). The color indicates the LogFC between Th0 and Th17 at the respective times.

autoimmune diseases and three non-autoimmune diseases, Alzheimer's disease, age-related macular degeneration and urinary incontinence as controls (Table 1). Autoimmune disease–associated SNPs were not enriched near early (0.5 h) Th17-specific enhancers, but the SNPs for ankylosing spondylitis, Crohn's disease, multiple sclerosis, polyendocrine syndromes, rheumatoid arthritis, systemic lupus erythematosus,

Table 1
SNPs associated with autoimmune diseases near Th17-specific enhancers are enriched.

Disease	Total SNPs	Th17 enhancers 0.5 h		Th17 enhancers 72 h	
		Overlapping SNPs	p-value	Overlapping SNPs	p-value
Ankylosing spondylitis (AS)	6736	2	0.77	36	0.013
Celiac disease (CD)	1931	2	0.67	14	0.072
Crohn's disease (CR)	11,197	0	1	64	0.009
IgA deficiency (IGA)	711	0	1	0	1
Multiple sclerosis (MS)	14,733	0	1	61	0.009
Primary biliary cholangitis (PBC)	2317	0	1	7	0.112
Polyendocrine syndrome (PS)	9793	1	0.84	45	0.009
Rheumatoid arthritis (RA)	11,832	3	0.77	68	<0.001
Systemic lupus erythematosus (SLE)	6739	0	1	26	0.047
Type 1 diabetes (T1D)	4513	0	1	14	0.112
Ulcerative colitis (UC)	9445	0	1	42	0.009
Urinary incontinence (UI)	117	0	1	0	1
Alzheimer's disease (AD)	29,775	0	1	56	0.364
Age-related macular degeneration (AMD)	14,882	0	1	26	0.509

and ulcerative colitis were enriched near late (72 h) Th17-specific enhancers. In contrast, SNPs associated with any of the non-autoimmune diseases were not enriched near Th17 specific enhancers at the two time points.

2.6. Regulatory SNPs within Th17-specific enhancers coincide with the TFBS of Th17-related TFs

A SNP occurring at TFBS can influence TF binding and thereby impact the transcription; such SNPs are often referred to as regulatory SNPs (rSNPs). Motivated by the observed enrichment of SNPs associated with autoimmune diseases in proximity to Th17-specific enhancers, we sought to ascertain whether these SNPs are situated within Th17 enhancers and whether they indeed coincide with a TFBS. To establish this overlap between a SNP and a TFBS, we set a proximity criterion of 15 bp between them.

Among the array of Th17-specific enhancers scrutinized, we identified 42 enhancers harbouring one or more rSNPs, totalling 104 rSNPs across these 42 enhancers (Table S4). Notably, within this set, 16 enhancers harbored 23 rSNPs that overlapped with a TFBS as observed in the ChIP-seq data for the respective transcription factor in T cells (Table 2, Table S4). The majority of these 23 rSNPs were located within late (72 h) enhancers, except for two rSNPs, rs1018326 and rs11678160, found within early (0.5 h) enhancers (Table S4). Notably, NFATC1, BATF, TBET, GATA3, HIC1, and STAT factors were the most prevalent TFs whose binding sites overlapped with rSNPs within Th17-specific enhancers (Table 2).

These 16 enhancers were in close proximity to genes implicated in T-cell function and autoimmunity, such as *CTLA4*, *CCL2*, *SLC30A7* (also known as Zinc transporter 7), and *SLC15A4*, an amino acid transporter crucial for interferon production [21]. Conversely, certain enhancer loci were near genes that have not been previously associated with T-cell function or autoimmunity, such as *LINC01934* and *LINC00423*.

We also tested if these 104 rSNPs have any *cis* or *trans* expression quantitative trait loci (eQTL) effects on gene expression in blood, leveraging the data from the eQTLGen consortium (https://eqtlgen.org/cis-eqtls.html) [22]. While 96 of the 104 rSNPs showed significant (FDR < 0.05) *cis*-eQTL effect on the expression of one or more of 135 genes (Table S5), the *trans*-eQTL effects were identified for only six rSNPs, impacting 35 genes. Notably, rs1003342 had a positive *trans*-eQTL effect on 20 genes, including *CCR7*, and a negative eQTL effect on

Table 2
Th17-specific enhancers containing disease-associated SNPs, which overlap the binding sites for TFs in ChIP-seq studies in T cells. Abbreviated disease name has been shown in the "diseases" column. For full name please see Table 1.

Enhancer locus	Target gene	SNP name	ref	alts	position	diseases	Overlapping TFs
chr1:100,946,801–100,961,200	SLC30A7	rs3903905	G	C,T,	chr1:100,955,401	MS; UC	GATA3
		rs17525451	A	G,	chr1:100,956,853	MS; UC	BATF; NFATC1; STAT4
chr2: 181,142,001–181,154,600	LINC01934/ ITGA4	rs1018326	T	A,C,G,	chr2:181,143,073	RA;AS;CD	NFATC1
chr2:203,840,001–203,844,600	CTLA4	rs13033315	A	G,T,	chr2:20,3842,142	CD; RA; T1D	STAT6
		rs231799	C	A,G,T,	chr2:203,842,694	RA	GABPA
		rs11571304	T	A,C,	chr2:203,844,053	CD; RA; T1D	NFATC1
chr2: 217,778,801–217,782,200	DIRC3	rs11678160	A	G,	chr2:217,780,257	RA	BATF
chr5:150,779,401–150,792,600	SMIM3	rs76767593	C	A,	chr5:150,790,281	AS; CR; PS; RA; UC	STAT3; STAT4
chr5:151,057,201–151,080,600	TNIP1	rs2233287	G	A,	chr5:151,060,536	RA	GATA3
		rs73272818	T	C,	chr5:151,065,282	RA	GATA3; TCF7
chr6:208,25,801–20,829,200	CDKAL1	rs4395717	C	A,G,	chr6:20,826,050	MS	ETS1; FLI1
chr6:167,031,001–167,032,200	FGFR1OP	rs2282859	T	C,G,	chr6:167,031,651	T1D	HIC1
chr10:62,742,001–62,743,800	ADO	rs224062	T	C,G,	chr10:62,743,036	CR; MS	NFATC1
chr12:128,801,601–128,803,000	SLC15A4	rs4760592	G	A,C,T,	chr12:128,802,604	SLE	BATF; FLI1
		rs10847691	G	A,	chr12:128,802,904	SLE	FLI1
chr13:32,916,401–32,918,800	LINC00423	rs6561636	G	A,	chr13:32,917,967	MS	BATF; GABPA
		rs4941702	G	A,C,T,	chr13:32,918,762	MS	HIC1
chr14:34,374,801–34,375,800	SPTSSA	rs1958589	T	C,	chr14:34,375,170	CD	HIC1
chr17:34,251,801–34,255,800	CCL2	rs2857656	G	A,C,	chr17:34,254,988	AS; CR; MS; PS; RA; UC	STAT4
chr17:47,618,601–47,621,800	KPNB1/ EFCAB13	rs4793978	G	A,	chr17:47,620,809	AS; CR; PS; RA; UC	STAT4; STAT5
chr20:32,751,801–32,754,200	COMMD7	rs6087989	A	G,T,	chr20:32,753,191	AS; CR; MS; PS; RA; UC	TBET
chr20:49,948,401–49,951,800	RNF114	rs144361842	C	G,T,	chr20:49,949,992	SLE	TBET
		rs2281217	C	A,G,T,	chr20:49,951,518	PS	HIC1

another five genes, including *TNFRSF4* (Table S5).

While each of those 23 rSNPs within the Th17-specific enhancers overlapping the binding sites of TFs in T cells had a *cis*-eQTL effect on one or more of 48 genes (Fig. 3), only one rSNP (rs1018326) had any *trans*-eQTL effect, which was on CCR9. Interestingly, three of the 23 rSNPs showed strong eQTL effect on CTLA4, suggesting that these rSNPs contribute to autoimmune disease susceptibility by regulating CTLA4 expression through the enhancer activity (Fig. 3). Furthermore, other genes impacted by these 23 rSNPs included several genes crucial for T-cell activation and autoimmunity, such as *CCL2*, *CCL8*, *CCR6*, *SLC30A7*, *SLC14A4*, *ICOS*, and *DNMT3B* (Fig. 3).

2.7. RORA locus harbors a super-enhancer specifically active in Th17 cells

Among the top Th17 enhancers was a SE region near RORA gene that has five ATAC-seq open loci and is located at the intronic region of the RORA isoform NM_134261.3 and upstream of other RORA isoforms (Fig. 4A; Table S1). The SE was specific to Th17 cells, particularly at 72 h (The highlighted region in Fig. 4A). The enhancers were clearly marked with H3K27ac mark in 72 h Th17 cells, but the mark was nearly absent in Th0 cells at 72 h and at early time in both cell types (Fig. S3A). H3K4me1 mark was similarly enriched in Th17 72 h cells, whereas H3K4me3 promoter mark was absent at the enhancer regions as expected (Fig. S3A).

Importantly, one of the five ATAC seq peaks in this SE overlapped a known enhancer region predicted to interact with RORA promoter (NM_134261.3) in GeneHancer database (Fig. 4A: GeneHancer track). The region was overlapping with encode conserved *cis*-regulatory element (cCREs). We tested whether this region (Marked as region #2 in Fig. 4B), the neighboring accessible regions (*i.e.*, regions #3 and #4) and the region devoid of ATAC-seq peak but overlapping the GeneHancer enhancer (*i.e.*, region #1) were functional. For this, we cloned these regions upstream of luciferase reporter gene of pGL4.10 plasmid construct and transfected to Th17 cells 72 h after initiation of differentiation. Th2 polarized (72 h) cells, served as controls, as we reported earlier [23]. Higher luciferase activity was detected in Th17 cells transfected with constructs containing open enhancer regions than in Th17 cells transfected with construct containing minimal promoter (Fig. 4C), suggesting that this enhancer positively regulates the transcription of the target gene. Interestingly, no increase in luciferase activity was detected in the construct containing region #1, suggesting that the region deficient in the ATAC peak was not functional. No luciferase activity was seen in Th2 cells in any of the clones (Fig. 4C).

2.8. Deletion of RORA enhancer leads to reduced RORA and IL17A expression

To further confirm the effect of the SE on RORA expression, we deleted a 270-bp TFBS-rich area (Fig. S3B), containing TFBSs for IRF4, MAF and STAT3 within region#2 (hg38:chr15:60,800,327-60,800,596), utilizing a plasmid-free CRISPR-Cas9 protocol that used an *in-vitro*-assembled *CRISPR-Cas9* complex in primary T cells (see Methods for details). Cells were nucleofected with either a pair of gRNA:Cas9 complex, where the two gRNAs (L4 and R4) were flanking the 270 bp-targeted genomic region (Fig. S4A), control non-targeting (NT) gRNA or control AAV1 gRNA. Interestingly, while PCR amplification of the NT-gRNA-treated sample generated a single band of the expected size, the sample treated with the L4/R4 gRNA pair generated two bands of which one was about 300 bp shorter (Fig. S4B). Sanger sequencing of DNA isolated from the generated PCR bands of the L4/R4 gRNA-treated sample showed that the targeted region was either completely deleted (Fig. S4C: middle panel: L4/R4-II) or changed containing insertions and deletions (Fig. S4C: upper panel: L4/R4-I), when compared to the sequence obtained from the NT/AAV1 gRNA-treated sample (Fig. S4C: lower two panels: NT-I and AAV1). Importantly, the CRISPR-Cas9-

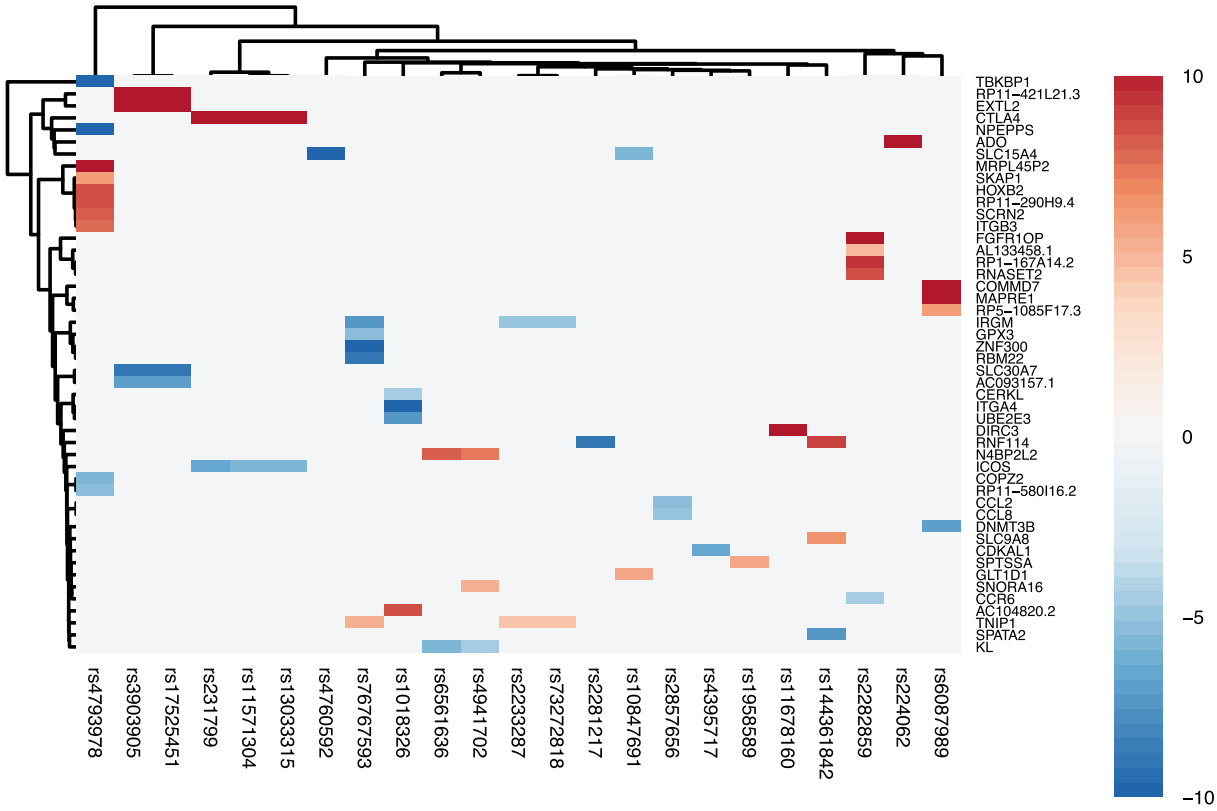

Fig. 3. *Cis*-eQTL effects of 23 SNPs that overlapped the binding sites of TFs shown in Table 2. The SNP eQTL data were taken from eQTLGen consortium [22]. The SNPs and genes have been clustered. The color shows the *Z*-score, and scales are capped to ±10.

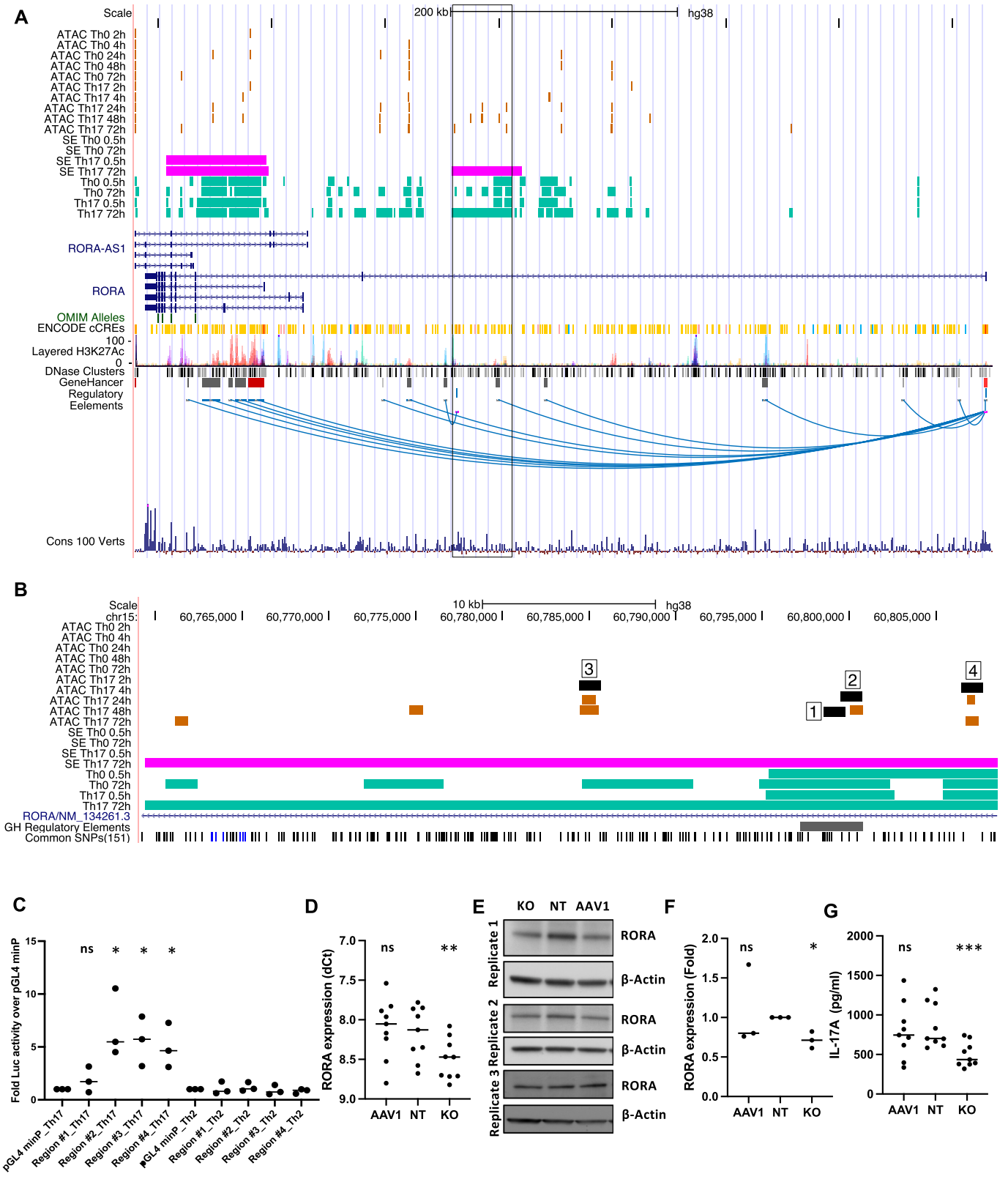

(caption on next page)

Fig. 4. RORA enhancer region and the effects of RORA enhancer deletion on the expression of RORA and IL-17A. (A) UCSC browser shots of RORA gene locus. The first five tracks show the ATAC-seq peaks at different time points of Th0 cells, followed by five tracks for Th17 cells. The next four tracks show super-enhancers, followed by four tracks for enhancers, in Th0 and Th17 cells at 0.5 and 72 h. GeneHancer tracks, including promoter-enhancer connections, are shown at the bottom. The portion highlighted by a rectangle is shown in panel B, which shows the four regions cloned upstream of firefly luciferase promoter in different plasmid constructs. (C) The graph shows the luciferase activity score when a construct containing one of the four regions shown in B was transfected in Th17 (72 h) or Th2 (72 h) cells. (D-G) The figures show the results obtained when a 270-bp TFBS-rich area of the enhancer region within region #2 has been deleted using CRISPR-Cas9. Please see methods for details. NT denotes samples treated with non-targeting gRNAs, and AAV1 denotes the samples treated with gRNAs targeting a safe harbor locus AAV1 to control for any effects of double-stranded breaks. The figures show the effect of deleting the enhancer (KO) on RORA RNA (D), RORA protein expression (E-F), and IL-17A secretion in culture supernatant (G), at 72 h. Panel E shows western blot images, and panel F shows its quantification data. In the univariate scatter plots (C, D, F, G), each dot is an individual biological replicate, and the horizontal lines show the means. Statistical significance was determined comparing each sample to pGL4_minP_Th17 to other samples in panel C and comparing KO and AAV to NT samples in panels D, F-G using two-tailed paired *t*-test. *:$p < 0.05$, **:$p < 0.01$, ***:$p < 0.001$, ns: not significant.

mediated DNA edition led to a decrease in expression of RORA RNA (Fig. 4D) and protein (Fig. 4E-F) and a significant decline in IL-17A production (Fig. 4G).

3. Discussion

By globally profiling histone marks H3K4me1, H3K4me3 and H3K27ac in conjunction with chromatin accessibility analysis, we meticulously charted the enhancer landscape of early Th17 differentiation in humans. Our investigation led to the identification of 23 rSNPs residing within Th17-specific enhancers. Notably, these rSNPs overlapped with the binding sites of TFs associated with T-cell function, thereby potentially exerting influence over TF binding and the subsequent expression of target genes. Importantly, we identified a Th17-specific enhancer region near RORA that played a crucial role in orchestrating the expression of RORA itself. To validate this regulatory role, we leveraged the power of CRISPR-Cas9-mediated deletion, targeting a region rich in TF binding sites within the RORA enhancer. Our experimental results confirmed the enhancer's direct involvement in modulating RORA transcription.

The precise mechanisms by which rSNPs in noncoding elements contribute to diverse phenotypes remain enigmatic. SNPs occurring at TFBSs may disrupt TF binding and alter gene transcription. Our previous work supported this notion by demonstrating that polymorphisms at TFBS indeed affect the binding of FOSL1/2 and BATF to their respective sites [24]. In the current study, we identified 23 autoimmune disease-associated rSNPs proximate to Th17-specific enhancers, and intriguingly, these rSNPs overlapped with the binding sites of T-cell-related TFs implicated in T-cell function, as elucidated through ChIP-seq studies specific to these TFs. This approach provides valuable insights into the potential mechanisms of action for SNPs located outside coding regions; however, it is contingent on the availability of ChIP-seq data for the specific TFs in T cells.

The 23 rSNPs within the Th17 specific enhancers have been associated with nine autoimmune diseases: multiple sclerosis, rheumatoid arthritis, type 1 diabetes, Crohn's disease, ulcerative colitis, celiac disease, ankylosing spondylitis, polyendocrine syndromes and systemic lupus erythematosus (Table 2), suggesting that these rSNPs may affect the function of associated enhancers thereby modulating Th17 response and thus influencing susceptibility to autoimmune diseases. For example, a risk variant (rs117701653) associated with type 1 diabetes and rheumatoid arthritis was shown to enhance the expression of inducible T cell co-stimulator (ICOS) by limiting the binding of chromosomal regulator SMCHD1 [25]. Further studies elucidating the mechanism of action of rSNPs that are localised in Th17-specific enhancers are likely to provide further understanding of pathogenesis of autoimmune diseases.

Enhancer establishment during the activation and differentiation of naive T cells into a specific lineage has been suggested to occur over days [26]. However, our investigation revealed that the differences in the enhancer landscape between Th0 and Th17 cells began to manifest already within 30 min into the differentiation process. Nonetheless, the early enhancers were not in proximity to known Th17 genes and did not harbor autoimmune disease-associated SNPs. In contrast, late enhancers (72 h) were strategically positioned near Th17 related genes, such as IL-17A, RORA, AHR, CCR2, CCR4, and CCR6, and notably hosted SNPs associated with autoimmune diseases.

Both RORα and RORγt promote Th17 differentiation, with RORγt being better characterized for its role during the process, including the role of histone methylation in the regulation of RORγt itself. Inhibiting histone H3K27 demethylases suppresses RORγt during Th17 differentiation [27]. Nonetheless, RORα is induced in Th17 cells in human [20] and mouse [7] and was identified as key Th17 promoting factor [7,9,14]. Further, RORα is required for a sustained *in vivo* Th17 response [28]. Interestingly, RORα was upregulated during human Th17 differentiation even before RORγt [20]. This raises the interesting possibility that RORα may have a more specific role in Th17 differentiation than RORγt, the latter being induced to a greater extent during human regulatory T-cell differentiation [29].

Studies conducted in mice have revealed that IRF4, in collaboration with BATF, an AP1 family TF, governs initial chromatin accessibility, and STAT3 instigates a specific transcriptional program during Th17 cell differentiation [7]. The enhancer region we studied harbors binding sites for AP1 factors as well as STAT3, suggesting that this enhancer facilitates early Th17 cell differentiation by recruiting these TFs at the promoter of RORA.

The integration of chromatin accessibility maps, TFBS enrichment analysis, and the enrichment of SNPs associated with autoimmune disease in proximity to enhancers provide improved understanding of early Th17 cell differentiation. Our study sheds light on a potential mechanism through which RORA enhancer and rSNPs located in the noncoding region contribute to the regulation of Th17 cell differentiation, ultimately influencing resistance or susceptibility to Th17 cell-mediated autoimmune pathologies.

4. Methods

4.1. T-cell isolation and differentiation

$CD4^+$ T cells were isolated from human umbilical cord blood using magnetic bead based positive selection as described [12]. $CD4^+$ T cells from multiple donors (three or more) were activated directly or pooled before activation with plate-bound anti-CD3 (3750 ng/6-well culture plate well) (Beckman Coulter, cat# IM-1304) and soluble anti-CD28 (1 μg/ml) (Beckman Coulter, cat# IM1376) at the density of 0.5×10^6 cells/ml of X-vivo 20 serum-free medium (Lonza, Bazel, Switzerland), supplemented with L-glutamine (2 mM, Sigma-Aldrich, Dorse, UK) and antibiotics (50 U/ml penicillin and 50 μg/ml streptomycin; Sigma-Aldrich). Th17 cell polarization was initiated with a cytokine cocktail of IL6 (20 ng/ml; Roche, cat# 11138600 001), IL1β (10 ng/ml, R&D Systems, cat# 201 LB) and TGFβ (10 ng/ml, R&D Systems, cat# 240) in the presence of neutralizing anti-IFNγ (1 μg/ml, R&D Systems, cat# MAB-285) and anti-IL4 (1 μg/ml, R&D Systems, cat# MAB204). For the control cells (Th0), CD4+ T cells were TCR stimulated with anti CD3 and anti CD28 in the presence of neutralizing antibodies without differentiating cytokines and cultured in parallel.

Th2 differentiation was performed as reported [30]. Briefly, CD4+ cells were activated with plate-bound anti-CD3 (500 ng/well, Beckman Coulter, #IM1304) and soluble anti-CD28 (500 ng/ml, #Beckman Coulter, #IM1376) at a density of 2–3 million cells/ml of Yssel's medium containing 1% human AB serum in presence of IL-4 (10 ng/ml, R&D Systems, #204-IL-050). At 48 h, IL-2 was added to the cultures (17 ng/ml, R&D Systems, #202-IL-500).

4.2. Luminex assay

Cytokines in the supernatant were measured by Luminex assay (Milliplex MAP human/mouse cytokine/chemokine magnetic bead panel; Luminex 200 by Luminex xMAP technology) according to the manufacturer's instructions. The concentrations were normalized using cell count data obtained by flow cytometry.

4.3. TaqMan assay

For RT-qPCR, RNA was isolated (RNeasy Mini Kit, #74106, QIAGEN) and treated in-column with DNase (RNase-Free Dnase Set, #79254, QIAGEN) for 15 min. The removal of genomic DNA was ascertained by treating the samples with DNase I (Invitrogen, #18068–015) before cDNA synthesis with SuperScript II Reverse Transcriptase (Invitrogen, #18064014). RT-qPCR was performed using KAPA Probe Fast Rox Low master mix (KAPA Biosystems, #kk4718) and amplification was monitored with QuantStudio 12 K Flex Real-Time PCR System (ThermoFisher Scientific). The Ct values were normalized against the signal acquired with EF1A. The following primers were used: IL17A (Forward: 5′-TGGGAAGACCTCATTGGTGT-3′and Reverse: 5′-GGATTTCGTGGGATTGTGAT-3′), RORA (ThermoFisher Scientific, Cat# 4331182, Assay ID: Hs00536545_m1), EF1A (Forward: 5′-AGCAAAAACGACCCACCA-3′and Reverse: 5′-GCCTGGATGGTTCAGGATAA-3′).

4.4. Western blotting

T cells were lysed using RIPA buffer (Pierce, Cat. no. 89901), supplemented with protease and phosphatase inhibitors (Roche) and sonicated using Bioruptor UCD-200 (Diagenode, Seraing, Belgium). Sonicated cell lysate was centrifuged at 14000 RPM for 20 min at 4 °C and supernatant was collected. Protein concentration of the sample was estimated by DC protein assay (BioRad) and heated with 6× Laemmli buffer at 96 °C for 5 min. Samples were loaded on gradient Mini-Protein TGX precast loading gel (BioRad) and transferred to PVDF membrane. The following antibodies were used: anti-RORα (Santa Cruz, sc-518,081), anti-β-Actin (Sigma, A5441) and HRP-conjugated anti-mouse IgG (Santa Cruz, sc-516,102) as secondary antibody.

4.5. ATAC-seq

Differentiating Th17 cells and respective Th0 cells from two donors were harvested at 0, 2, 4, 24, 48, and 72 h. ATAC-seq libraries were prepared as described [23]. Amplified libraries were purified by double SPRI beads purifications. 0.4× beads:DNA ratio for the first time, flow through was kept (removing large fragments); 1.4× beads:DNA ratio for the second time, beads were kept. Libraries were eluted from the beads by elution in 20 μl of Buffer EB (from QIAGEN PCR Purification Kit). A 1-μl library was run on a Agilent Bioanalyzer to check size distribution and quality of the libraries. Sequencing was done with an Illumina Hiseq 2500.

All samples were sequenced in all lanes to remove lane-specific batch effects. Read quality control was performed with FastQC (v.0.11.4). The adapter sequences present in the raw reads were trimmed using TrimGalore! (v. 0.4.5), and the trimmed reads were mapped to the hg38 reference genome using Bowtie2 (v. 2.3.3.1). Duplicate reads were marked with Picard tools' (v. 2.17.8) MarkDuplicates function. Narrow peaks were called using MACS2 (v. 2.1.0), and reproducible peaks present in both replicates were identified using IDR with an FDR cut-off of 0.05. To enable comparison between the samples, a union of the reproducible peaks present in all samples was defined as a complete set of features. The featureCounts method from the Rsubread R package was used to assign reads to the genomic regions. The raw count data were normalized using the TMM method. Identification of differentially accessible genomic regions was performed with R package Limma using the normalized count data as input. Genomic regions with a fold-change >2 and FDR ≤ 0.01 were defined as differentially accessible. The genomic regions were annotated using HOMER (v.4.9).

4.6. ChIP-seq

Cells were activated under Th0 and Th17 condition for 0.5 and 72 h. ChIP assay was performed using H3K4me1 (Diagenode, C15410194), H3K4me3 (Diagenode, C15410003) and H3K27ac (Diagenode, C15410196) antibodies as described [29]. The quality of the raw data was checked with FastQC (v.0.11.3) [31] and MultiQC (v.1.5) [32]. The library complexity for all the samples fulfilled the quality criteria recommended by ENCODE. The reads were aligned to hg38 reference genome using Bowtie [33]. Most samples had around 20 million uniquely mapped reads. Cross correlation analysis [34,35] found an enrichment in all the antibody samples but not in any input samples, suggesting that ChIP experiments were successful. Library complexity was determined with preseq (v.2.0.3) [36]. Only reads of mapping quality >30 were used in the downstream analysis. Duplicates were removed with Picard tools (Picard), and samples were then downsampled to the median depth.

4.7. Identification of enhancers and super-enhancers

Enhancers were predicted with ChromHMM (v.1.20) [16] with five chromatin states. Two result states were manually defined to correspond to weak and strong enhancers and were included in the subsequent analysis. For predicting SEs, ROSE (v.0.1) [17] was used with H3K27ac as ranking signal. To identify enhancers unique to a cell type (Th0 or Th17) or stage of differentiation (0.5 h or 72 h), we used MAnorm (v.1.1.4). We preferred MAnorm over bedtools-based subtractions because the former also provides statistical measures of confidence. Log2FC > 0.6 and $p < 0.01$ cut off were used for significance. Enhancers from different replicates were merged such that the enhancers that were found in at least two replicates were retained, and their boundaries were the union of all the replicates where the enhancer was found.

4.8. Transcription factor binding site analysis

Overrepresentation of TFBSs on the enhancers was examined using the FMatch tool at the TRANSFAC database. A randomly generated gene set of approximately the same size was taken as a background for calculating overrepresentation. A custom profile was generated where we only took matrices corresponding to the TFs expressed in T cells during early differentiation [20,29]: 658 motifs. The enrichment was calculated using binomial test. The *p*-value was corrected by the Benjamin & Hochberg method in r (version 4.2.1). FDR < 0.05 was considered significant.

4.9. SNP enrichment analysis

SNP enrichment analysis was performed with snpEnrichR (v.0.0.1) R package. For SNP enrichment analysis, disease-associated SNPs, we used disease-associated SNPs from NHGRI-EBI GWAS catalogue or ImmunoChip database. SNPs from studies with meta-analysis of more than one disease and from populations other than Caucasian were excluded from further analysis, and correlated SNPs were clumped (distance = 1000 kb, LD r2 = 0.8). Random SNP sets matching the disease-associated SNPs were produced using SNPsnap server with default parameters except

distance = 1000 kb, LD buddies ±20%, r2 = 0.8. Proxy SNPs for both disease-associated and random SNPs were calculated using Plink (v1.90b6.27) from 1000 genomes EUR population.

The enrichment null distributions are assessed by counting the overlaps of SNPs with random locations of size equal to enhancer sets from the genome with 1000-fold repetition. The overlap method excludes the telomeres and centromeres as they are not known to hold any regulatory sites. SNPs overlapping known transcription factor motifs were identified using annotatePeaks.pl from Homer (v.4.10). Motifs were searched within a 30-bp region around each SNP coordinate. For the heatmap visualising the cis-eQTL effects of the SNPs overlapping TFBS, Euclidean distances of both rows and column were clustered using Ward's minimum variance method.

4.10. Luciferase assay

The Dual-Luciferase Reporter Assay was performed as described (Khan et al. 2022). Briefly, CD4+ cells were polarized to Th2 (used as control) and Th17 cells for 72 h and transiently nucleofected with a promoter-luciferase reporter pGL4.10 plasmid (Promega). After 48 h resting, the cells were reactivated under Th2 and Th17 conditions for 24 h, harvested in passive lysate buffer (provided in the Dual-Luciferase Reporter Assay from Promega, cat# E1910) and luciferase activity was measured according to the manufacturer's instructions. In each sample, firefly luciferase values were normalized to values of pGL4.74 renilla luciferase plasmid and plotted as a fold-change over empty luciferase construct pGL4-minP. Plasmids containing the RORA enhancer region were synthesized commercially by GeneScript.

4.11. CRISPR-Cas9-mediated DNA edition

Guide RNAs (gRNAs) were *in-vitro*-assembled with the *Cas9* protein as described [37]. Briefly, crisprRNA (crRNA)s, designed using CRISPETa design tool [38] and synthesized by IDT (https://eu.idtdna.com), and tracrRNA (Alt-R CRISPR-Cas9 tracrRNA, #1072533, IDT) were reconstituted to 160 M and combined in equimolar amounts (1:1) and incubated at 37 °C for 30 min to prepare 80 μM gRNA reagent. Assembled gRNA was then mixed with an equal volume of 40 μM recombinant *S. pyogenes* Cas9-nuclear localization sequence (NLS) purified protein (QB3 MacroLab, University of California, Berkeley) (giving 2:1 gRNA to Cas9 molar ratio) together with 1 μL of 100 μM non-homologous single-strand DNA enhancer (ssODNenh, synthesized by IDT), and incubated for 10 min at 37 °C for a final concentration of 20 μM CRISPR-Cas9 ribonucleoprotein (RNP).

For genomic DNA deletion, a pair of gRNA:Cas9 complex (prepared as described above using crRNA-L4: 5′- ACTGCTCTCTGCTAGCCTGG −3′ and crRNA-R4: 5′-TGGTCTATAGCCAGGACACT-3′) was used. For control cells, non-targeting (NT) gRNA:Cas9 complex or a gRNA:Cas9 complex targeting a safe harbor locus, were respectively prepared by using a negative control crRNA (NC1 from IDT: 5′-CGTTAATCGCGTATAATACG-3′) or AAVS1–670 crRNA (IDT: 5′-CCTCTAAGGTTTGCTTACGA-3′). Freshly purified $CD4^+$ cells (4×10^6 cells) were then transfected by nucleofection with the RNP complexes and rested for 24 h in RPMI supplemented with 10% serum and further cultured under Th17 conditions, as described above.

At 72 h after cell activation, 80 μl of the cells was collected, and DNA was extracted (using Quick Extract DNA Extraction Solution 1.0, #QE09050, Epicentre) and used to PCR amplify a 885-bp genomic region, including the CRISPR targeted region, with the following primers (Forward: 5′-AGCCAGGGCTGTGTTATTC-3′and Reverse: 5′-ACTAACTG-CAGCCCAACATAG-3′) and using KAPA HiFi HotStart PCR Kit (#KR0369, Roche). Generated PCR products were analyzed on 1.2% agarose gel, bands were cut out, and DNA was extracted (GeneJET Gel Extraction Kit (#K0691, ThermoFisher Scientific) its concentration determined (NanoDrop 2000, ThermoFisher Scientific). Purified PCR DNA products were then analyzed by Sanger sequencing (carried out at FIMM Sequencing laboratory, University of Helsinki, Finland) with the following primer (5′-GACACGCTGTTCCACTTAATT-3′).

Supplementary data to this article can be found online at https://doi.org/10.1016/j.clim.2024.110261.

Ethical approval

Ethics Committee of Hospital District of Southwest Finland approved usage of the blood of unknown donors.

Author contributions

UUK designed and performed experiments, analyzed data, prepared figures and wrote the manuscript; RB designed and performed experiments, analyzed data, prepared figures and wrote the manuscript; SJ analyzed data, prepared figures and contributed to writing; MMK designed and performed experiments, analyzed data and prepared figures; ST designed experiments, set up and optimized a range of methods and generated preliminary data that guided the further study design; MHK designed and performed the experiments, analyzed data, and prepared figures; JS, KK, TE, AL analyzed data and prepared figures; AM contributed to CRISPR experiments. OR designed the experiments, analyzed the data, and wrote the manuscript; LE provided scientific expertise and feedback on the manuscript; RL designed and supervised the study and wrote the manuscript.

CRediT authorship contribution statement

Ubaid Ullah Kalim: Writing – review & editing, Writing – original draft, Visualization, Supervision, Project administration, Investigation, Formal analysis, Data curation. **Rahul Biradar:** Writing – review & editing, Methodology, Investigation. **Sini Junttila:** Writing – review & editing, Writing – original draft, Visualization, Supervision, Methodology, Investigation, Formal analysis. **Mohd Moin Khan:** Writing – review & editing, Visualization, Methodology, Investigation, Formal analysis. **Subhash Tripathi:** Writing – review & editing, Project administration, Methodology, Investigation. **Meraj Hasan Khan:** Writing – review & editing, Methodology, Investigation. **Johannes Smolander:** Writing – review & editing, Methodology, Investigation. **Kartiek Kanduri:** Writing – review & editing, Methodology, Investigation, Formal analysis. **Tapio Envall:** Writing – review & editing, Methodology. **Asta Laiho:** Writing – review & editing, Methodology. **Alexander Marson:** Writing – review & editing, Resources, Methodology, Investigation. **Omid Rasool:** Writing – review & editing, Writing – original draft, Visualization, Supervision, Resources, Methodology, Investigation. **Laura L. Elo:** Writing – review & editing, Visualization, Supervision, Resources, Project administration, Methodology, Investigation, Funding acquisition. **Riitta Lahesmaa:** Writing – review & editing, Writing – original draft, Supervision, Resources, Project administration, Investigation, Funding acquisition, Conceptualization.

Declaration of generative AI and AI-assisted technologies in the writing process

During the preparation of this work the authors used ChatGPT 3.5 in order to improve readability. After using this tool, the authors reviewed and edited the content as needed and take full responsibility for the content of the publication.

Declaration of competing interest

Alexander Marson is a co-founder of Arsenal Biosciences, Spotlight Therapeutics, and Survey Genomics, serves on the boards of directors at Spotlight Therapeutics and Survey Genomics, is a board observer (and former member of the board of directors) at Arsenal Biosciences, is a member of the scientific advisory boards of Arsenal Biosciences,

Spotlight Therapeutics, Survey Genomics, NewLimit, Amgen, Tenaya, and Lightcast, owns stock in Arsenal Biosciences, Spotlight Therapeutics, NewLimit, Survey Genomics, PACT Pharma, Tenaya, and Lightcast, and has received fees from Arsenal Biosciences, Spotlight Therapeutics, NewLimit, 23andMe, PACT Pharma, Juno Therapeutics, Tenaya, Lightcast, Trizell, Vertex, Merck, Amgen, Genentech, AlphaSights, Rupert Case Management, Bernstein, and ALDA. A.M. is an investor in and informal advisor to Offline Ventures and a client of EPIQ. The Marson laboratory has received research support from Juno Therapeutics, Epinomics, Sanofi, GlaxoSmithKline, Gilead, and Anthem. All other authors declare no competing interests.

The ChIP-seq and ATAC-seq raw and processed data has been submitted to GEO and can be accessed with the following super-series accession number: GSE243064.

Data availability

The ChIP-seq and ATAC-seq raw and processed data has been submitted to GEO and can be accessed with the following super-series accession number GSE243064.

Acknowledgements

We thank the staff of Turku University Hospital, Department of Obstetrics and Gynecology, Maternity Ward, for the cord blood collection. We also thank Marjo Hakkarainen and Sarita Heinonen for excellent technical help. We also duly acknowledge core facilities at the department namely, the Finnish Functional Genomics Centre and Cell Imaging Core facility supported by Biocenter Finland. The Finnish Centre for Scientific Computing is duly acknowledged for their efficient servers and their resources in data analysis. MMK was supported by University of Turku graduate school on Turku Doctoral Programme of Molecular Medicine (TuDMM) as well as a central grant from Finnish Cultural Foundation. RL was supported by the Academy of Finland, Centre of Excellence in Molecular Systems Immunology and Physiology Research (2012-2017) grant 250114; by the Academy of Finland grants 292335, 294337, 292482, 31444, by grants from the JDRF and the Finnish Cancer Foundation, the Novo Nordisk Foundation grant NNF19OC0057218 and the Jane and Aatos Erkko Foundation grant. LLE was supported by European Research Council ERC 677943 European Union's Horizon 2020 research and innovation programme 955321, Academy of Finland grants 310561, 314443, 329278, 335434, 335611 and 341342. RL and LLE were supported by the Sigrid Jusélius Foundation, Turku Graduate School University of Turku, Åbo Akademi University, InFLAMES Flagship Programme of the Academy of Finland 337530, Biocenter Finland and ELIXIR Finland.

References

[1] T. Korn, E. Bettelli, M. Oukka, V.K. Kuchroo, IL-17 and Th17 cells, Annu. Rev. Immunol. 27 (2009) 485–517, https://doi.org/10.1146/annurev.immunol.021908.132710.

[2] M. Veldhoen, R.J. Hocking, C.J. Atkins, R.M. Locksley, B. Stockinger, TGFbeta in the context of an inflammatory cytokine milieu supports de novo differentiation of IL-17-producing T cells, Immunity 24 (2006) 179–189, https://doi.org/10.1016/j.immuni.2006.01.001.

[3] P.R. Mangan, L.E. Harrington, D.B. O'Quinn, W.S. Helms, D.C. Bullard, C.O. Elson, R.D. Hatton, S.M. Wahl, T.R. Schoeb, C.T. Weaver, Transforming growth factor-beta induces development of the T(H)17 lineage, Nature 441 (2006) 231–234, https://doi.org/10.1038/nature04754.

[4] E. Bettelli, Y. Carrier, W. Gao, T. Korn, T.B. Strom, M. Oukka, H.L. Weiner, V. K. Kuchroo, Reciprocal developmental pathways for the generation of pathogenic effector TH17 and regulatory T cells, Nature 441 (2006) 235–238, https://doi.org/10.1038/nature04753.

[5] D.J. Cua, J. Sherlock, Y. Chen, C.A. Murphy, B. Joyce, B. Seymour, L. Lucian, W. To, S. Kwan, T. Churakova, S. Zurawski, M. Wiekowski, S.A. Lira, D. Gorman, R. A. Kastelein, J.D. Sedgwick, Interleukin-23 rather than interleukin-12 is the critical cytokine for autoimmune inflammation of the brain, Nature 421 (2003) 744–748, https://doi.org/10.1038/nature01355.

[6] C.T. Weaver, L.E. Harrington, P.R. Mangan, M. Gavrieli, K.M. Murphy, Th17: an effector CD4 T cell lineage with regulatory T cell ties, Immunity 24 (2006) 677–688, https://doi.org/10.1016/j.immuni.2006.06.002.

[7] M. Ciofani, A. Madar, C. Galan, M. Sellars, K. MacE, F. Pauli, A. Agarwal, W. Huang, C.N. Parkurst, M. Muratet, K.M. Newberry, S. Meadows, A. Greenfield, Y. Yang, P. Jain, F.K. Kirigin, C. Birchmeier, E.F. Wagner, K.M. Murphy, R. M. Myers, R. Bonneau, D.R. Littman, A validated regulatory network for Th17 cell specification, Cell 151 (2012) 289–303, https://doi.org/10.1016/j.cell.2012.09.016.

[8] Z. Fang, K. Hecklau, F. Gross, I. Bachmann, M. Venzke, M. Karl, J. Schuchhardt, A. Radbruch, H. Herzel, R. Baumgrass, Transcription factor co-occupied regions in the murine genome constitute T-helper-cell subtype-specific enhancers, Eur. J. Immunol. 45 (2015) 3150–3157, https://doi.org/10.1002/eji.201545713.

[9] E.R. Miraldi, M. Pokrovskii, A. Watters, D.M. Castro, N. De Veaux, J.A. Hall, J. Y. Lee, M. Ciofani, A. Madar, N. Carriero, D.R. Littman, R. Bonneau, Leveraging chromatin accessibility for transcriptional regulatory network inference in T helper 17 cells, Genome Res. 29 (2019) 449–463, https://doi.org/10.1101/gr.238253.118.

[10] Y. Tian, C. Han, Z. Wei, H. Dong, X. Shen, Y. Cui, X. Fu, Z. Tian, S. Wang, J. Zhou, D. Yang, Y. Sun, J. Yuan, B. Ni, Y. Wu, SOX-5 activates a novel RORγt enhancer to facilitate experimental autoimmune encephalomyelitis by promoting Th17 cell differentiation, Nat. Commun. 12 (2021) 1–18, https://doi.org/10.1038/s41467-020-20786-w.

[11] D. Lara-Astiaso, A. Weiner, E. Lorenzo-Vivas, I. Zaretsky, D.A. Jaitin, E. David, H. Keren-Shaul, A. Mildner, D. Winter, S. Jung, N. Friedman, I. Amit, Chromatin state dynamics during blood formation, Science 55 (2014) 1–10, https://doi.org/10.1126/science.1256271.

[12] R.D. Hawkins, A. Larjo, S.K. Tripathi, U. Wagner, Y. Luu, T. Lönnberg, S.K. Raghav, L.K. Lee, R. Lund, B. Ren, H. Lähdesmäki, R. Lahesmaa, Global chromatin state analysis reveals lineage-specific enhancers during the initiation of human T helper 1 and T helper 2 cell polarization, Immunity 38 (2013) 1271–1284, https://doi.org/10.1016/j.immuni.2013.05.011.

[13] V. Kumar, H.-J. Westra, J. Karjalainen, D.V. Zhernakova, T. Esko, B. Hrdlickova, R. Almeida, A. Zhernakova, E. Reinmaa, U. Võsa, M.H. Hofker, R.S.N. Fehrmann, J. Fu, S. Withoff, A. Metspalu, L. Franke, C. Wijmenga, Human disease-associated genetic variation impacts large intergenic non-coding RNA expression, PLoS Genet. 9 (2013) e1003201, https://doi.org/10.1371/journal.pgen.1003201.

[14] X.O. Yang, B.P. Pappu, R. Nurieva, A. Akimzhanov, H.S. Kang, Y. Chung, L. Ma, B. Shah, A.D. Panopoulos, K.S. Schluns, S.S. Watowich, Q. Tian, A.M. Jetten, C. Dong, T helper 17 lineage differentiation is programmed by orphan nuclear receptors RORα and RORγ, Immunity 28 (2008) 29–39, https://doi.org/10.1016/j.immuni.2007.11.016.

[15] G. Castro, X. Liu, K. Ngo, A. De Leon-tabaldo, S. Zhao, R. Luna-roman, J. Yu, T. Cao, R. Kuhn, P. Wilkinson, K. Herman, M.I. Nelen, J. Blevitt, X. Xue, A. Fourie, P. Fung-leung, ROR γ t and ROR α signature genes in human, PLOS ONE (2017) 1–22.

[16] J. Ernst, M. Kellis, Chromatin-state discovery and genome annotation with ChromHMM, Nat. Protoc. 12 (2017) 2478–2492, https://doi.org/10.1038/nprot.2017.124.

[17] W.A. Whyte, D.A. Orlando, D. Hnisz, B.J. Abraham, C.Y. Lin, M.H. Kagey, P. B. Rahl, T.I. Lee, R.A. Young, Master transcription factors and mediator establish super-enhancers at key cell identity genes, Cell 153 (2013) 307–319, https://doi.org/10.1016/j.cell.2013.03.035.

[18] M. Boyd, M. Thodberg, M. Vitezic, J. Bornholdt, K. Vitting-Seerup, Y. Chen, M. Coskun, Y. Li, B.Z.S. Lo, P. Klausen, P. Jan Schweiger, A.G. Pedersen, N. Rapin, K. Skovgaard, K. Dahlgaard, R. Andersson, T.B. Terkelsen, B. Lilje, J.T. Troelsen, A. M. Petersen, K.B. Jensen, I. Gögenur, P. Thielsen, J.B. Seidelin, O.H. Nielsen, J. T. Bjerrum, A. Sandelin, Characterization of the enhancer and promoter landscape of inflammatory bowel disease from human colon biopsies, Nat. Commun. 9 (2018), https://doi.org/10.1038/s41467-018-03766-z.

[19] S. Fishilevich, R. Nudel, N. Rappaport, R. Hadar, I. Plaschkes, T. Iny Stein, N. Rosen, A. Kohn, M. Twik, M. Safran, D. Lancet, D. Cohen, GeneHancer: genome-wide integration of enhancers and target genes in GeneCards, Database (Oxford) 2017 (2017) 1–17, https://doi.org/10.1093/database/bax028.

[20] S. Tuomela, S. Rautio, H. Ahlfors, V. Öling, V. Salo, Comparative analysis of human and mouse transcriptomes of Th17 cell priming, Oncotarget 7 (2016) 13416–13428.

[21] T. Kobayashi, D. Nguyen-Tien, D. Ohshima, H. Karyu, S. Shimabukuro-Demoto, R. Yoshida-Sugitani, N. Toyama-Sorimachi, Human SLC15A4 is crucial for TLR-mediated type i interferon production and mitochondrial integrity, Int. Immunol. 33 (2021) 399–406, https://doi.org/10.1093/intimm/dxab006.

[22] U. Võsa, A. Claringbould, H.J. Westra, M.J. Bonder, P. Deelen, B. Zeng, H. Kirsten, A. Saha, R. Kreuzhuber, S. Yazar, H. Brugge, R. Oelen, D.H. de Vries, M.G.P. van der Wijst, S. Kasela, N. Pervjakova, I. Alves, M.J. Favé, M. Agbessi, M. W. Christiansen, R. Jansen, I. Seppälä, L. Tong, A. Teumer, K. Schramm, G. Hemani, J. Verlouw, H. Yaghootkar, R. Sönmez Flitman, A. Brown, V. Kukushkina, A. Kalnapenkis, S. Rüeger, E. Porcu, J. Kronberg, J. Kettunen, B. Lee, F. Zhang, T. Qi, J.A. Hernandez, W. Arindrarto, F. Beutner, J. Dmitrieva, M. Elansary, B.P. Fairfax, M. Georges, B.T. Heijmans, A.W. Hewitt, M. Kähönen, Y. Kim, J.C. Knight, P. Kovacs, K. Krohn, S. Li, M. Loeffler, U.M. Marigorta, H. Mei, Y. Momozawa, M. Müller-Nurasyid, M. Nauck, M.G. Nivard, B.W.J.H. Penninx, J. K. Pritchard, O.T. Raitakari, O. Rotzschke, E.P. Slagboom, C.D.A. Stehouwer, M. Stumvoll, P. Sullivan, P.A.C. 't Hoen, J. Thiery, A. Tönjes, J. van Dongen, M. van Iterson, J.H. Veldink, U. Völker, R. Warmerdam, C. Wijmenga, M. Swertz, A. Andiappan, G.W. Montgomery, S. Ripatti, M. Perola, Z. Kutalik, E. Dermitzakis, S. Bergmann, T. Frayling, J. van Meurs, H. Prokisch, H. Ahsan, B.L. Pierce,

T. Lehtimäki, D.I. Boomsma, B.M. Psaty, S.A. Gharib, P. Awadalla, L. Milani, W. H. Ouwehand, K. Downes, O. Stegle, A. Battle, P.M. Visscher, J. Yang, M. Scholz, J. Powell, G. Gibson, T. Esko, L. Franke, Large-scale cis- and trans-eQTL analyses identify thousands of genetic loci and polygenic scores that regulate blood gene expression, Nat. Genet. 53 (2021) 1300–1310, https://doi.org/10.1038/s41588-021-00913-z.

[23] M.M. Khan, M.H. Khan, U.U. Kalim, Long intergenic noncoding RNA MIAT as a regulator of human Th17 cell differentiation, Front. Immunol. 13 (2022) 1–14, https://doi.org/10.3389/fimmu.2022.856762.

[24] A. Shetty, S.K. Tripathi, S. Junttila, T. Buchacher, R. Biradar, S.D. Bhosale, T. Envall, A. Laiho, R. Moulder, O. Rasool, S. Galande, L.L. Elo, R. Lahesmaa, A systematic comparison of FOSL1, FOSL2 and BATF-mediated transcriptional regulation during early human Th17 differentiation, Nucleic Acids Res. 50 (2022) 4938–4958, https://doi.org/10.1093/nar/gkac256.

[25] T. Kim, M. Martínez-Bonet, Q. Wang, N. Hackert, J.A. Sparks, Y. Baglaenko, B. Koh, R. Darbousset, R. Laza-Briviesca, X. Chen, V.R.C. Aguiar, D.J. Chiu, H.J. Westra, M. Gutierrez-Arcelus, M.T. Weirauch, S. Raychaudhuri, D.A. Rao, P.A. Nigrovic, Non-coding autoimmune risk variant defines role for ICOS in T peripheral helper cell development, Nat. Commun. 15 (2024) 1–14, https://doi.org/10.1038/s41467-024-46457-8.

[26] K.M. Ansel, I. Djuretic, B. Tanasa, A. Rao, Regulation of TH2 differentiation and Il4 locus accessibility, Annu. Rev. Immunol. 24 (2006) 607–656, https://doi.org/10.1146/annurev.immunol.23.021704.115821.

[27] A.P. Cribbs, S. Terlecki-Zaniewicz, M. Philpott, J. Baardman, D. Ahern, M. Lindow, S. Obad, H. Oerum, B. Sampey, P.K. Mander, H. Penn, P. Wordsworth, P. Bowness, M. de Winther, R.K. Prinjha, M. Feldmann, U. Oppermann, Histone H3K27me3 demethylases regulate human Th17 cell development and effector functions by impacting on metabolism, Proc. Natl. Acad. Sci. U. S. A. 117 (2020) 6056–6066, https://doi.org/10.1073/pnas.1919893117.

[28] J.A. Hall, M. Pokrovskii, L. Kroehling, B.R. Kim, S.Y. Kim, L. Wu, J.Y. Lee, D. R. Littman, Transcription factor RORα enforces stability of the Th17 cell effector program by binding to a Rorc cis-regulatory element, Immunity 55 (2022) 2027–2043.e9, https://doi.org/10.1016/j.immuni.2022.09.013.

[29] U. Ullah, S.B.A. Andrabi, S.K. Tripathi, O. Dirasantha, K. Kanduri, S. Rautio, C. C. Gross, S. Lehtimäki, K. Bala, J. Tuomisto, U. Bhatia, D. Chakroborty, L.L. Elo, H. Lähdesmäki, H. Wiendl, O. Rasool, R. Lahesmaa, Transcriptional repressor HIC1 contributes to suppressive function of human induced regulatory T cells, Cell Rep. 22 (2018) 2094–2106, https://doi.org/10.1016/j.celrep.2018.01.070.

[30] J. Henriksson, X. Chen, T. Gomes, U. Ullah, K.B. Meyer, R. Miragaia, G. Duddy, J. Pramanik, K. Yusa, R. Lahesmaa, S.A. Teichmann, Genome-wide CRISPR screens in T helper cells reveal pervasive crosstalk between activation and differentiation, Cell 176 (2019) 882–896.e18, https://doi.org/10.1016/j.cell.2018.11.044.

[31] S. Andrews, FastQC: A Quality Control Tool for High Throughput Sequence Data [Online], Available online at, http://www.bioinformatics.babraham.ac.uk/projects/fastqc/, 2010, https://qubeshub.org/resources/fastqc.

[32] P. Ewels, M. Magnusson, S. Lundin, M. Käller, MultiQC: summarize analysis results for multiple tools and samples in a single report, Bioinformatics 32 (2016) 3047–3048, https://doi.org/10.1093/bioinformatics/btw354.

[33] B. Langmead, S.L. Salzberg, Fast gapped-read alignment with bowtie 2, Nat. Methods 9 (2012) 357–359.

[34] P.V. Kharchenko, M.Y. Tolstorukov, P.J. Park, Design and analysis of ChIP-seq experiments for DNA-binding proteins, Nat. Biotechnol. 26 (2008) 1351–1359, https://doi.org/10.1038/nbt.1508.

[35] S.G. Landt, G.K. Marinov, A. Kundaje, P. Kheradpour, F. Pauli, S. Batzoglou, B. E. Bernstein, P. Bickel, J.B. Brown, P. Cayting, Y. Chen, G. DeSalvo, C. Epstein, K. I. Fisher-Aylor, G. Euskirchen, M. Gerstein, J. Gertz, A.J. Hartemink, M. M. Hoffman, V.R. Iyer, Y.L. Jung, S. Karmakar, M. Kellis, P.V. Kharchenko, Q. Li, T. Liu, X.S. Liu, L. Ma, A. Milosavljevic, R.M. Myers, P.J. Park, M.J. Pazin, M. D. Perry, D. Raha, T.E. Reddy, J. Rozowsky, N. Shoresh, A. Sidow, M. Slattery, J. A. Stamatoyannopoulos, M.Y. Tolstorukov, K.P. White, S. Xi, P.J. Farnham, J. D. Lieb, B.J. Wold, M. Snyder, ChIP-seq guidelines and practices of the ENCODE and modENCODE consortia, Genome Res. 22 (2012) 1813–1831, https://doi.org/10.1101/gr.136184.111.

[36] T. Daley, A.D. Smith, Predicting the molecular complexity of sequencing libraries, Nat. Methods 10 (2013) 325–327, https://doi.org/10.1038/nmeth.2375.

[37] T.L. Roth, C. Puig-Saus, R. Yu, E. Shifrut, J. Carnevale, P.J. Li, J. Hiatt, J. Saco, P. Krystofinski, H. Li, V. Tobin, D.N. Nguyen, M.R. Lee, A.L. Putnam, A.L. Ferris, J. W. Chen, J.N. Schickel, L. Pellerin, D. Carmody, G. Alkorta-Aranburu, D. Del Gaudio, H. Matsumoto, M. Morell, Y. Mao, M. Cho, R.M. Quadros, C. B. Gurumurthy, B. Smith, M. Haugwitz, S.H. Hughes, J.S. Weissman, K. Schumann, J.H. Esensten, A.P. May, A. Ashworth, G.M. Kupfer, S.A.W. Greeley, R. Bacchetta, E. Meffre, M.G. Roncarolo, N. Romberg, K.C. Herold, A. Ribas, M.D. Leonetti, A. Marson, Reprogramming human T cell function and specificity with non-viral genome targeting, Nature 559 (2018) 405–409, https://doi.org/10.1038/s41586-018-0326-5.

[38] C. Pulido-Quetglas, E. Aparicio-Prat, C. Arnan, T. Polidori, T. Hermoso, E. Palumbo, J. Ponomarenko, R. Guigo, R. Johnson, Scalable Design of Paired CRISPR guide RNAs for genomic deletion, PLoS Comput. Biol. 13 (2017) 1–18, https://doi.org/10.1371/journal.pcbi.1005341.